Available online at www.sciencedirect.com
ScienceDirect
Journal of Magnetic Resonance 187 (2007) 44–51
JMR Journal of Magnetic Resonance
www.elsevier.com/locate/jmr

Transient NOE-exchange-relay experiment: Application to ligand–protein binding under slow exchange conditions

I.S. Podkorytov, N.R. Skrynnikov *

Department of Chemistry, Purdue University, 560 Oval Drive, West Lafayette, IN 47907-2084, USA

Received 3 November 2006; revised 11 February 2007
Available online 24 March 2007

Abstract

A new version of one-dimensional ^{1}H experiment has been developed to probe ligand binding to macromolecular targets. The experiment, called transient NOE-exchange relay, is similar to the 'reverse NOE pumping' technique [A. Chen, M.J. Shapiro, J. Am. Chem. Soc. 122 (2000) 414–415]. The T_2 filter is used to erase protein magnetization, and the saturation then spreads from protein to bound ligand (via NOE) and further to a free ligand (via on–off exchange). The ligand signals, monitored as a function of mixing time, present a familiar 'dip' pattern characteristic of transient NOE or transient exchange experiments. In addition to the T_2 filter, we have also implemented a T_1 filter which makes use of the fact that the selective T_1^{-1} rates in macromolecules are much higher than those in small ligands. To model the experiment, complete relaxation and exchange matrix analysis has been invoked. This formalism was further used as a starting point to develop a simplified treatment where the relaxation and exchange components are represented by 2×2 matrix and, in addition, there is a special term responsible for coupling of ligand magnetization to the protein spin bath. The proposed experimental scheme has been tested on a system of peanut agglutinin complexed with Me-β-D-galactopyranoside, which is known to be in a slow exchange regime. The results suggest that the NOE-exchange-relay experiment can be used at the advanced stages of the drug development process to confirm high-affinity ligand binding.

Keywords: Ligand–protein binding; Transient NOE-exchange-relay experiment; NMR screening; Reverse NOE pumping; Saturation transfer difference; Peanut agglutinin

1. Introduction

NMR spectroscopy proved to be a useful screening tool for identification of small molecules that bind to macromolecular targets [1–4]. In the process of drug development, NMR-based screen initially identifies a small number of compounds with modest binding affinity. Based on the obtained results, working compound libraries are constructed in a more focused manner to search for ligands with higher binding affinities. During this iterative procedure, NMR serves as one of the important binding assays. A number of homo- and heteronuclear pulse sequences have been developed with this purpose in mind.

Transient NOE [5] and transient exchange [6] experiments are part of a standard NMR toolkit. In these experiments one component of a spin system is selectively excited; the perturbation then propagates through the system, carried by Overhauser effect or by chemical exchange. Here we describe a simple variant of this experiment where the perturbation is transmitted in a relayed fashion: from a large protein to its bound ligand via NOE and farther on to the pool of free ligand molecules via chemical exchange. Conceptually, the experiment bears strong similarity to the saturation transfer difference experiment [7] and especially to the reverse NOE pumping experiment [8]. Of note, closely related methods have been also developed in the field of magnetic resonance imaging [9,10]. Our specific experimental scheme, however, is distinct from the commonly used differential spectroscopy approaches.

* Corresponding author. Fax: +1 765 494 0239.
E-mail address: nikolai@purdue.edu (N.R. Skrynnikov).

1090-7807/$ - see front matter © 2007 Elsevier Inc. All rights reserved.
doi:10.1016/j.jmr.2007.02.016

To analyze the proposed experimental scheme we conducted complete relaxation and exchange matrix analysis [11–13]. We further found a way to simplify this treatment, reducing it to a system of two differential equations. Using the simplified approach, we explored the range of applicability of NOE-exchange-relay experiments. So far practical applications of this class of experiments have been limited to the case of weak binding/fast exchange. We found that such measurements can be also carried out under slow exchange conditions. This has been confirmed experimentally for the model system of peanut agglutinin complexed with Me-β-D-galactopyranoside. The slow exchange in this case plays a role of a limiting step in the NOE-exchange relay. It is envisioned that the described measurement scheme can be helpful at the advanced stages of the screening process where it can be used to identify compounds with relatively tight binding, $K_d < 1$ μM, and exclude false positives [14,15].

2. Pulse sequence

The sequence shown in Fig. 1a is designed for mixture of small ligand and large macromolecular target. The first T_2 filter nullifies the magnetization associated with the protein, while preserving the magnetization of the free ligand (in effect, the filter achieves saturation of the protein magnetization). During the mixing time, τ_{mix}, saturation is transferred from the protein onto a bound ligand and further to the free ligand, causing a decrease in the amount of magnetization associated with the free ligand. As τ_{mix} becomes longer, T_1 relaxation takes over, and the free ligand magnetization is restored to its equilibrium value. The observed signal, taken as a function of τ_{mix}, displays therefore a 'dip' pattern characteristic of transient NOE and transient exchange measurements [5,6].

Prior to the detection, the system is subjected to the second T_2 filter. The purpose of this filter is to eliminate the broad protein background which builds up during the time τ_{mix}. Finally, the 3-9-19 element [16] is inserted in the sequence to suppress the residual HDO signal (the measurements are conducted in D_2O solvent).

Fig. 1b shows a variant of this sequence where the starting T_2 filter is replaced with a T_1 filter. The new filter takes advantage of large selective T_1^{-1} relaxation rates in a big protein. In the presented application, the ligand is a simple monosaccharide with proton resonances lying downfield of 3.4 ppm. The starting selective 180° pulse, of i-SNOB variety [17], inverts the entire spectrum of the ligand as well as portion of the protein spectrum, but not the protein methyl or methylene resonances. Subsequently, during the time τ_1, inverted protein magnetization rapidly recovers (the selective character of protein relaxation is ensured by the presence of unperturbed methyl/methylene magnetization [18]). On the other hand, the magnetization of the free ligand does not change substantially over the same time period. At this point, the application of a hard 180° pulse creates the state where ligand magnetization is close to equilibrium, whereas protein magnetization is, in a good approximation, inverted. The advantage of this preparation scheme is that a uniform (even if incomplete) inversion is achieved for all protons in the protein. The remaining part of the sequence, beginning with τ_{mix}, is identical to Fig. 1a.

3. Theory

For the two-component system at hand, spin evolution during the mixing time τ_{mix} is described by the following system of equations:

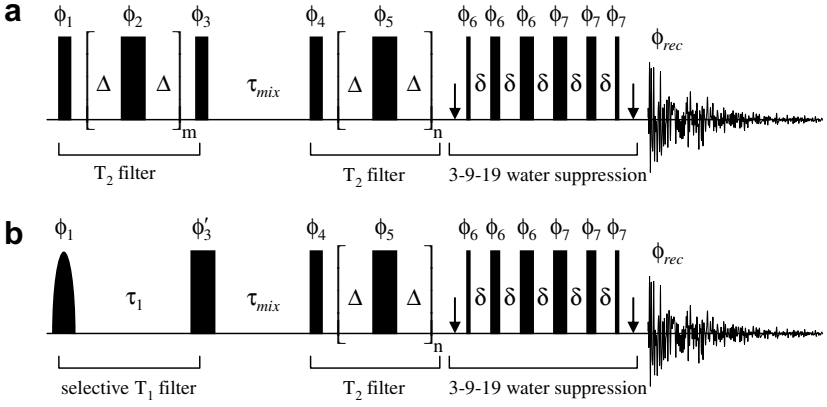

Fig. 1. Transient NOE-exchange-relay experiments. The CPMG T_2 filters are applied with $\Delta = 1$ ms, $m = 10$, $n = 44$. The water suppression element, which serves to eliminate the residual HDO signal, employs (3π/26)–(9π/26)–(19π/26)–(19π/26)–(9π/26)–(3π/26) pulse train [16] with interpulse separation $\delta = 0.37$ ms. Arrows denote the application of sine-bell shaped gradients with duration of 1 ms and amplitude of 10 G/cm. The (excessive) phase cycling is $\phi_1 = -\phi_3 = x$, $\phi_2 = 32(y)32(-y)$, $\phi_4 = 8(x)8(y)8(-x)8(-y)$, $\phi_5 = 4(y)4(-y)4(-x)4(x)4(-y)4(y)4(x)4(-x)$, $\phi_6 = -\phi_7 = 16(x,y,-x,-y)$, $\phi_{rec} = 4(x,-x)4(-y,y)4(-x,x)4(y,-y)$. The variant of the sequence shown in (b) begins with i-SNOB-2 pulse [17] applied at the center of the ligand spectrum, 3.68 ppm, with the duration of 3.3 ms and the power of 0.73 kHz. The subsequent delay τ_1, at the core of the selective T_1 filter, is 50 ms. The phase cycle is identical to the sequence (a), with the exception of $\phi_3' = 32(x)32(y)32(-x)32(-y)$.

$$\frac{\mathrm{d}}{\mathrm{d}t}m_i^{\mathrm{lf}} = -km_i^{\mathrm{lf}} + km_i^{\mathrm{lb}} - \sum_{j=1}^{N_{\mathrm{l}}} R_{ij}^{\mathrm{lf,lf}}(m_j^{\mathrm{lf}} - 1) \tag{1.1}$$

$$\frac{\mathrm{d}}{\mathrm{d}t}m_i^{\mathrm{lb}} = k_{\mathrm{off}}m_i^{\mathrm{lf}} - k_{\mathrm{off}}m_i^{\mathrm{lb}} - \sum_{j=1}^{N_{\mathrm{l}}} R_{\mathrm{ij}}^{\mathrm{lb,lb}}(m_j^{\mathrm{lb}} - 1) - \sum_{s=1}^{N_p} R_{is}^{\mathrm{lb,pb}}(m_s^{\mathrm{pb}} - 1) \tag{1.2}$$

$$\frac{\mathrm{d}}{\mathrm{d}t}m_q^{\mathrm{pf}} = -\tilde{k}m_q^{\mathrm{pf}} + \tilde{k}m_q^{\mathrm{pb}} - \sum_{s=1}^{N_{\mathrm{p}}} R_{qs}^{\mathrm{pf,pf}}(m_s^{\mathrm{pf}} - 1) \tag{1.3}$$

$$\frac{\mathrm{d}}{\mathrm{d}t}m_q^{\mathrm{pb}} = k_{\mathrm{off}}m_q^{\mathrm{pf}} - k_{\mathrm{off}}m_q^{\mathrm{pb}} - \sum_{s=1}^{N_{\mathrm{p}}} R_{qs}^{\mathrm{pb,pb}}(m_s^{\mathrm{pb}} - 1) - \sum_{j=1}^{N_l} R_{qj}^{\mathrm{pb,lb}}(m_j^{\mathrm{lb}} - 1). \tag{1.4}$$

Here m_i^{lf} and m_i^{lb} denote magnetization associated with the ith proton from the ligand ($i = 1, \ldots, N_{\mathrm{l}}$) in the free and bound states, respectively. Likewise, m_q^{pf} and m_q^{pb} denote magnetization associated with the qth proton from the protein ($q = 1, \ldots, N_{\mathrm{p}}$) in the free and bound states. All magnetizations are defined so that their equilibrium value is 1. The exchange rates are k_{off}, $k = k_{\mathrm{on}}[\mathrm{P}]$, and $\tilde{k} = k_{\mathrm{on}}[\mathrm{L}]$, with [P] and [L] representing the concentrations of the free protein and free ligand in solution. Finally, R is the Redfield relaxation matrix, including both auto- and cross-relaxation. Of particular importance are the elements $R_{is}^{\mathrm{lb,pb}}$ representing intermolecular NOE coupling in the ligand-protein complex. Eqs. (1.1)–(1.4) are formulated within the framework of complete relaxation and exchange matrix analysis [11–13] where the spin density matrix is represented by single spin operators only. Indeed, it can be demonstrated that three-spin orders arising due to dipole–dipolar cross-correlated cross-relaxation are relatively unimportant in this context [19].

It is worth noting that complete relaxation matrix analyses has had limited success in quantifying ^{1}H relaxation rates. This is due to uncertainty in interproton distances, which is significant even in high-resolution protein structures, and to the lack of information on internal dynamics, especially with regard to methyl groups that play the role of "relaxation sinks" [20]. Hence, Eqs. (1.1)–(1.4) provide, at best, a semi-quantitative description for the problem at hand. In this situation it is logical to search for a simplified treatment that would be more revealing than Eqs. (1.1)–(1.4), yet retain a semi-quantitative accuracy.

In deriving a trimmed-down version of Eqs. (1.1)–(1.4) we made several simplifying assumptions. First, due to the very large size of the ^{1}H spin reservoir, protein relaxation is insensitive to the presence of small ligand. Furthermore, due to spin diffusion, protons tend to relax with similar effective rates [21]. Hence, we postulated that protein ^{1}H relaxation can be modeled as generic exponential decay, and the following substitution can be made in Eq. (1.2)

$$(m_s^{\mathrm{pb}} - 1) = (m^{\mathrm{p}}(0) - 1)\exp(-\Gamma^{\mathrm{p}}t) \tag{2}$$

$$\Gamma^{\mathrm{p}} = \frac{1}{N_{\mathrm{p}}}\sum_{q=1}^{N_{\mathrm{p}}}\left\{\sum_{s=1}^{N_{\mathrm{p}}} R_{qs}^{\mathrm{pf,pf}}\right\}. \tag{3}$$

Here $m^p(0)$ and Γ^p are, respectively, the initial state and the relaxation rate constant of generalized ^{1}H spin that models the protein spin bath. In calculating Γ^p, Eq. (3), the inner summation obtains non-selective relaxation rates for an individual proton q (expression in curly brackets) [22]. This result can be gleaned from Eq. (1.3) if one assumes that all m_s^{pf} are equal and can be replaced with m_q^{pf}. The outer summation obtains the average over all protons.

Second, we assume that m_j^{lf} ($j = 1 \ldots, N_{\mathrm{l}}$) appearing on the r.h.s. of Eq. (1.1) are all equal and can be replaced with m_i^{lf} (likewise, m_j^{lb} in Eq. (1.2) can be replaced with m_i^{lb}). Once again, this approach leads to non-selective relaxation rates for like spins [23]. Indeed, for the considered class of experiments the relaxation within the free ligand, as well as the bound ligand, has non-selective character.

The result is the system of differential equations for ligand magnetization:

$$\frac{\mathrm{d}}{\mathrm{d}t}m_i^{\mathrm{lf}} = -km_i^{\mathrm{lf}} + km_i^{\mathrm{lb}} - \Gamma_i^{\mathrm{lf}}(m_i^{\mathrm{lf}} - 1) \tag{4.1}$$

$$\frac{\mathrm{d}}{\mathrm{d}t}m_i^{\mathrm{lb}} = k_{\mathrm{off}}m_i^{\mathrm{lf}} - k_{\mathrm{off}}m_i^{\mathrm{lb}} - \Gamma_i^{\mathrm{lb}}(m_i^{\mathrm{lb}} - 1) - \Gamma_i^{\mathrm{lb,pb}}(m^{\mathrm{p}}(0) - 1)\exp(-\Gamma^{\mathrm{p}}t) \tag{4.2}$$

where

$$\Gamma_i^{\mathrm{lf}} = \sum_{j=1}^{N_{\mathrm{l}}} R_{ij}^{\mathrm{lf,lf}}, \quad \Gamma_i^{\mathrm{lb}} = \sum_{j=1}^{N_{\mathrm{l}}} R_{ij}^{\mathrm{lb,lb}}, \quad \text{and}$$

$$\Gamma_i^{\mathrm{lb,pb}} = \sum_{s=1}^{N_{\mathrm{p}}} R_{is}^{\mathrm{lb,pb}}. \tag{5}$$

Eqs. (4.1) and (4.2) can be written for each individual proton of the ligand, resulting in the system of *two* equations per proton. The last term in Eq. (4.2), which stands for NOE coupling to the protein bath, makes the equation inhomogeneous. The analytical solution for this system of equations is readily available, but unwieldy. Alternatively, the equations can be integrated numerically. The physical meaning of Eqs. (4.1) and (4.2) is transparent: they describe a trivial case of spin relaxation in the presence of two-site exchange (cf. Bloch–McConnell equation [24]), *plus* coupling of ligand magnetization to protein spin bath via the intermolecular NOE in the ligand–protein complex. Analogous equations can be set up for transverse magnetization; in this case, the coupling term $\Gamma_i^{\mathrm{lb,pb}}$ is normally assumed to be zero due to the difference in precession frequencies of individual protons.

For the sake of completeness we consider the limiting case of fast exchange, $k + k_{\mathrm{off}} \gg \Gamma$. First, a standard basis transformation can be applied to Eqs. (4.1) and (4.2): $m_i^{\Sigma} = c^{\mathrm{lf}}m_i^{\mathrm{lf}} + c^{\mathrm{lb}}m_i^{\mathrm{lb}}$ and $m_i^{\Delta} = m_i^{\mathrm{lf}} - m_i^{\mathrm{lb}}$, where $c^{\mathrm{lf}} = [\mathrm{L}]/[\mathrm{L}_0] = k_{\mathrm{off}}/(k + k_{\mathrm{off}})$ and $c^{\mathrm{lb}} = 1 - c^{\mathrm{lf}}$ are the fractions of free and bound ligand, respectively. Second, it is noted that

m_i^{Δ} is rapidly destroyed by exchange and, therefore, can be set to zero in the analyses. The result for the observable m_i^{Σ} is

$$\frac{\mathrm{d}}{\mathrm{d}t}m_i^{\Sigma} = -\bar{\Gamma}_i^{\mathrm{l}}(m_i^{\Sigma}-1) - c^{\mathrm{lb}}\Gamma_i^{\mathrm{lb,pb}}(m^{\mathrm{p}}(0)-1)\exp(-\Gamma^{\mathrm{p}}t) \quad (6)$$

where $\bar{\Gamma}_i^{\mathrm{l}} = c^{\mathrm{lf}}\Gamma_i^{\mathrm{lf}} + c^{\mathrm{lb}}\Gamma_i^{\mathrm{lb}}$. The solution to this equation is

$$m_i^{\Sigma}(t) = 1 + (m_i^{\Sigma}(0)-1)\exp(-\bar{\Gamma}_i^{\mathrm{l}}t) + c^{\mathrm{lb}}\Gamma_i^{\mathrm{lb,pb}}(m^{\mathrm{p}}(0)-1)\frac{\exp(-\Gamma^{\mathrm{p}}t)-\exp(-\bar{\Gamma}_i^{\mathrm{l}}t)}{\Gamma^{\mathrm{p}}-\bar{\Gamma}_i^{\mathrm{l}}}. \quad (7)$$

This curve may have an extremum at

$$t_{\mathrm{e}} = \frac{1}{\bar{\Gamma}_i^{\mathrm{l}}-\Gamma^{\mathrm{p}}}\ln\left\{\frac{\bar{\Gamma}_i^{\mathrm{l}}}{\Gamma^{\mathrm{p}}}\left(1+\frac{(\bar{\Gamma}_i^{\mathrm{l}}-\Gamma^{\mathrm{p}})}{c^{\mathrm{lb}}\Gamma_i^{\mathrm{lb,pb}}}\frac{(m_{\mathrm{i}}^{\Sigma}(0)-1)}{(m^{\mathrm{p}}(0)-1)}\right)\right\}. \quad (8)$$

For a protein–ligand complex where the intermolecular NOE is negative ($\Gamma^{\mathrm{lb,pb}} < 0$) Eq. (8) defines a minimum of the characteristic 'dipping' curve. This result is relevant for most of the weakly binding ligands, including a number of model systems investigated in the past [7,8].

4. Experimental results

The proposed experimental scheme has been tested using the sample of peanut agglutinin complexed with Me-β-D-galactopyranoside (MBG). This system has been quantitatively studied before and the kinetic constants at 25 °C were determined to be $k_{\mathrm{off}} = 40\ \mathrm{s}^{-1}$ and $k_{\mathrm{on}} = 4\times10^4\ \mathrm{M}^{-1}\ \mathrm{s}^{-1}$ [25]. To demonstrate the NOE-exchange-relay experiment, the sample with equimolar concentration (0.17 mM) of agglutinin and MBG has been prepared. Under these conditions, the expected association rate is $k = 6\ \mathrm{s}^{-1}$ and the exchange rate, $k_{\mathrm{ex}} = k + k_{\mathrm{off}}$, is reasonably slow.

A series of one-dimensional proton spectra have been recorded using the pulse sequences shown in Fig. 1a and b for fourteen τ_{mix} delays in the range from 0 to 3 s. In addition, the reference experiment was recorded with $\tau_{\mathrm{mix}} = 10$ s. The signals from individual MBG protons were integrated and normalized according to $I_i(\tau_{\mathrm{mix}})/I_i(\infty)$, where $I_i(\infty) = I_i(\tau_{\mathrm{mix}} = 10\ \mathrm{s})$. The results are presented in Fig. 2.

For better visualization, the continuous curves have been added to the plots in Fig. 2. To generate these curves, the experimental points for each proton were fitted using Eqs. (4.1) and (4.2) with the maximum number of adjustable parameters (two exchange rate constants, four relaxation terms, and three magnetization amplitudes representing the initial conditions). While this procedure is evidently prone to overfitting, it demonstrates that the simplified model, Eqs. (4.1) and (4.2), can readily accommodate the experimental data.

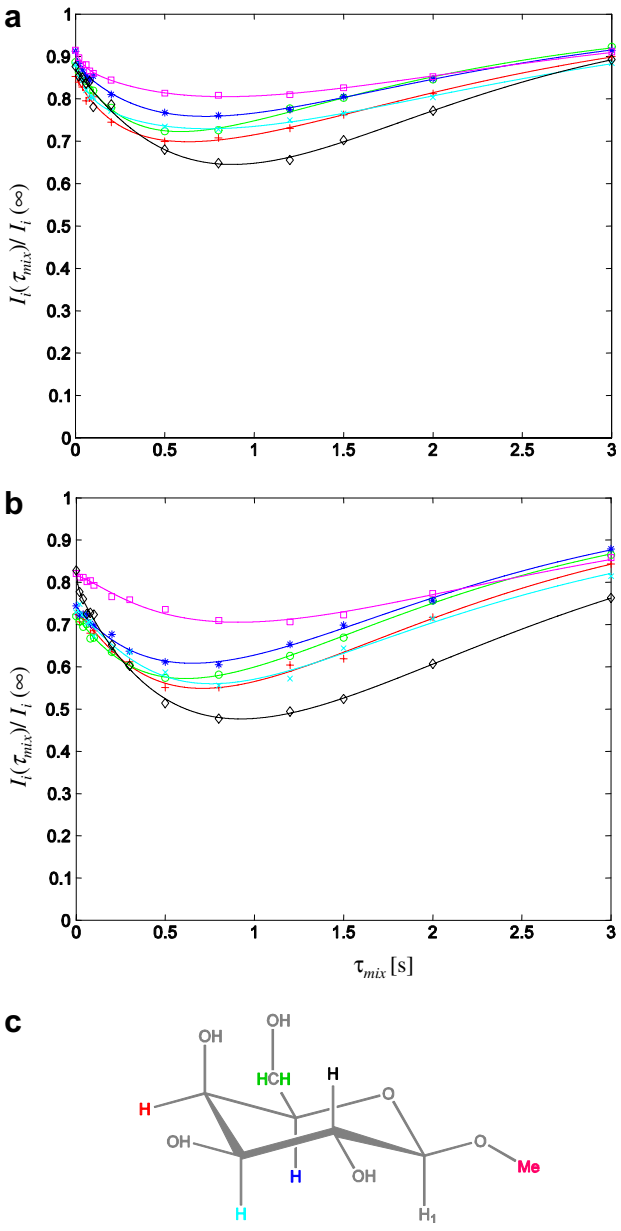

Fig. 2. Intensities of ligand signals, $I_i(\tau_{\mathrm{mix}})/I_i(\infty)$, measured with pulse sequences (a) Fig. 1a and (b) Fig. 1b. The sample conditions were 0.17 mM peanut agglutinin (concentration determined spectrophotometrically [26]; under current conditions the protein forms a tetramer with 110 kDa net weight), 0.17 mM MBG, D_2O-based phosphate buffer [25], 23 °C. The spectra were recorded overnight (400 scans per τ_{mix} point with the recycling delay 5.5 s) on a 500 MHz Bruker Avance DRX-500 spectrometer equipped with triple-resonance probe and z-gradient unit. The MBG signals were integrated using XWIN-NMR [27]; the data are color-coded as shown in panel (c). The continuous curves were generated by fitting the experimental data to Eqs. (4.1) and (4.2) as described in the text. The fitting procedure assumed that observable signals are represented by m_i^{lf} (characteristic of the slow exchange regime) rather than $m_i^{\Sigma} = c^{\mathrm{lf}}m_i^{\mathrm{lf}} + c^{\mathrm{lb}}m_i^{\mathrm{lb}}$ (fast exchange limit). A special series of line-shape simulations established that this is indeed the case for the system at hand.

5. Simulations

To validate our interpretation of the experiment Fig. 1, we carried out a series of numeric simulations. First, the complete relaxation and exchange matrix analysis has been performed based on Eqs. (1.1)–(1.4). The exchange rates were used as reported by Neurohr et al. [25]. The relaxation rates

were calculated using the crystallographic structure PDB ID 1QF3 [28] (the structure was protonated using the HyperChem software [29] assuming that all exchangeable protons are replaced with deuterium). Proton–proton dipolar and proton CSA interactions were taken into consideration in calculating the relaxation matrix elements. In addition, a small contribution from paramagnetic O_2 into the auto-relaxation rates, 0.05 s^{-1}, was included [30]. The proton CSA tensor was assumed to be axially symmetric with unique axis along the CH bond and the anisotropy of 10 ppm [31]. Local dynamics has been neglected with the important exception of the methyl groups [13,20]. In the case of methyls, the Lipari–Szabo-type spectral densities have been used with the order parameter of 1/9 for the CSA interaction and 1/4 for proton–proton dipolar interactions within the methyl group [32]. The local correlation time was set to 40 ps for protein side-chain methyls [33] and to 10 ps for methoxy methyl in MBG (in the latter case, the estimate was based on analogy with methionine side chains). For dipolar interactions between methyl protons and the protons outside the given methyl group order parameter was set to 1 and the relaxation rates were computed using the average coordinates of the three methyl protons. The overall tumbling time for free MBG in D_2O at 23 °C was taken to be 60 ps [34] and the overall tumbling time of agglutinin tetramer under the same conditions was estimated to be 65 ns [35]. In the interests of computation speed, the simulations were limited to a single agglutinin molecule with bound MBG, resulting in the 2656×2656 relaxation and exchange matrix (additional tests showed that this is more than sufficient to model a large spin reservoir associated with the tetramer). The simulations were designed to cover the entire length of the pulse sequence Fig. 1a, including the two filter elements. The quantity $m_i^{\mathrm{lf}}(\tau_{\mathrm{mix}})/m_i^{\mathrm{lf}}(\infty)$ was taken to be the observable. The results of this comprehensive simulation are presented in Fig. 3a.

As a next step, the complete relaxation and exchange matrix was resummed as described in Section 3 and the system of Eqs. (4.1) and (4.2) was set up for each of the MBG protons. Equations analogous to (4.1) and (4.2) were also formulated to describe the spin evolution during the T_2 filters. The equations were then integrated numerically, with the output shown in Fig. 3b.

Comparison of Figs. 3a and 2a shows that the simulations do remarkably well in reproducing the experimental trends on a per-atom basis. In particular, the substantial effect involving methylene protons (green curve) is well reproduced despite recently expressed misgivings concerning their higher auto-relaxation rates [13,36]. This brings up the question as to whether the results can be used to characterize the binding mode of the ligand, i.e. for the epitope mapping. The conventional wisdom holds that under slow exchange conditions the protons in the bound ligand become all equilibrated with the protein spin bath and therefore can no longer be distinguished [37]. To address this aspect, we investigated the flow of saturation in the complex of agglutinin with MBG. The simulations showed that with the present off-rate, $k_{\mathrm{off}} = 40\ s^{-1}$, it is in

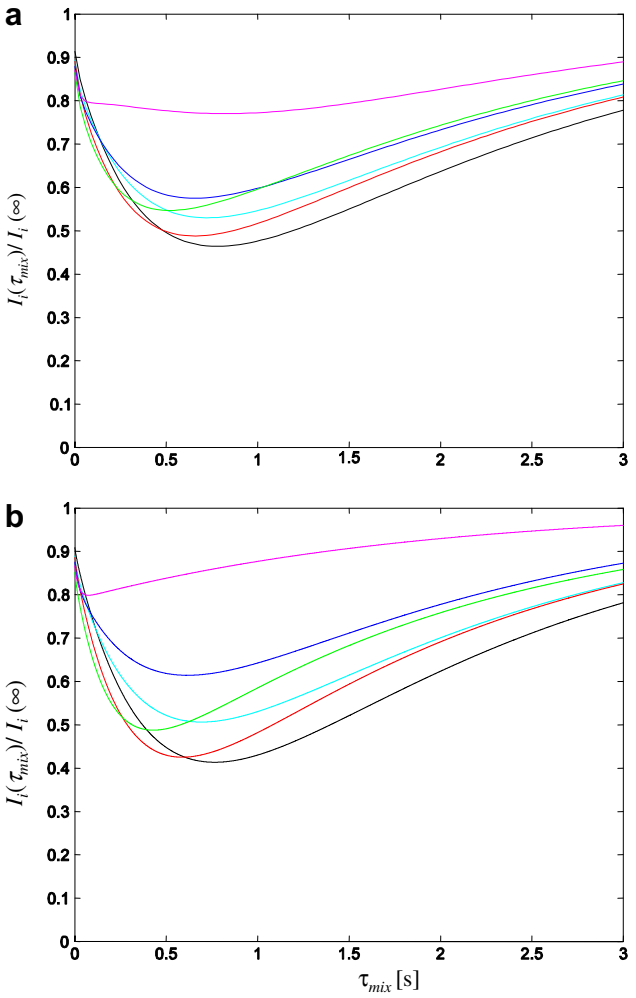

Fig. 3. Simulated intensities of ligand signals, $I_i(\tau_{\mathrm{mix}})/I_i(\infty)$, generated by means of complete relaxation and exchange matrix analysis (a) and the simplified treatment, Eqs. (4.1) and (4.2) (b).

principle possible to differentiate between the protons in MBG. In practice, however, only the methoxy group stands out: it extends outward into solvent and shows the smallest transient NOE effect (magenta symbols in Figs. 3a and 2a). For other protons in this small ligand there is no simple way (short of the complete relaxation and exchange matrix analysis) to translate the experimental data into the epitope information. Finally, our simulations indicate that for truly slow k_{off} rates, $k_{\mathrm{off}} \sim 1\ s^{-1}$, the magnetizations of individual protons in the bound ligand are indeed equalized and the epitope mapping is no longer possible.

While the simulations proved to be remarkably accurate in reproducing the experimental trends, the truly quantitative agreement is lacking (cf. Figs. 3a and 2a). This is not surprising given the limitations of the computational model. A number of parameters used in our simulations are poorly known: for example, k_{on} carries the uncertainty of 30% [25] and a similarly large uncertainty is associated with rotational correlation time of the agglutinin tetramer [35]. Comparison of Figs. 3a and 2a suggests that the proton recovery rates are substantially underestimated by the

simulations. Indeed, the mean simulated value for non-selective proton relaxation rate in agglutinin is $I^{\mathrm{p}} = 0.6\ \mathrm{s}^{-1}$. In fact, the rate is ca. $1.0\ \mathrm{s}^{-1}$, typical of large proteins in D_2O solvent at room temperature [38]. This discrepancy is probably due to a relatively crude character of the model with respect to internal protein dynamics: for instance, the model does not account for side-chain rotameric jumps [39] which can contribute to proton relaxation. The discrepancies such as this can indeed explain the lack of quantitative accuracy in the simulation results.

Given the imprecise character of the complete relaxation and exchange matrix analysis, we anticipate that the approximate treatment based on Eqs. (4.1) and (4.2) may provide a comparably accurate model. Indeed, Fig. 3b generated on the basis of Eqs. (4.1) and (4.2) displays the same features as observed in Fig. 3a; the deviations between the two graphs are relatively small. The approximate treatment therefore opens the door for rapid semi-quantitative analysis of the NOE-exchange-relay experiments.

6. Range of applicability

We have used Eqs. (4.1) and (4.2) to model the NOE-exchange-relay effect under different exchange conditions. In doing so, we retained the spin topology and the effective relaxation rate constants of the MBG-agglutinin system. The composition of the sample and the exchange parameters, on the other hand, were varied. To characterize the outcome of the measurements we determined the depth of the 'dip', i.e. the difference between the starting and the lowest point of the curve: $m_i^{\mathrm{lf}}(0) - m_i^{\mathrm{lf}}(\tau_{\mathrm{mix}}^{\mathrm{min}})$ in the case of slow exchange and $m_i^{\Sigma}(0) - m_i^{\Sigma}(\tau_{\mathrm{mix}}^{\mathrm{min}})$ in the case of fast exchange. Of all MBG protons, the one with the deepest 'dip' has been chosen to represent the magnitude of the effect. The representative results are illustrated in Fig. 4.

The two characteristic cases presented in Fig. 4a and b correspond to slow and fast exchange regimes, respectively. Fig. 4b illustrates the situation relevant for initial NMR screening that identifies lead compounds with modest binding affinity to a protein target (dissociation constant 1 mM has been used in the simulations). This case has been the primary objective of the experiments by Chen and Shapiro [8] and Mayer and Meyer [7]. Fig. 4a, on the other hand, illustrates the case of tight binding (dissociation constant 10 nM) which has not been as extensively investigated in pharmaceutically oriented NMR. The plot demonstrates that the 'dipping' curve can be readily obtained in this case for a broad range of samples (2- to 10-fold ligand excess). The effect seems particularly useful since binding produces only a small amount of line-broadening, $k = 1$–$0.1\ \mathrm{s}^{-1}$, under these circumstances. The exchange kinetics illustrated in Fig. 4a is similar to that in the experimentally studied MBG–agglutinin complex. However, the on-rate used in the simulation, $k_{\mathrm{on}} = 10^8\ \mathrm{M}^{-1}\ \mathrm{s}^{-1}$, is more typical of pharmaceutically active ligands binding to protein targets. These results suggest that the transient NOE-exchange-relay experiments can confirm the binding events

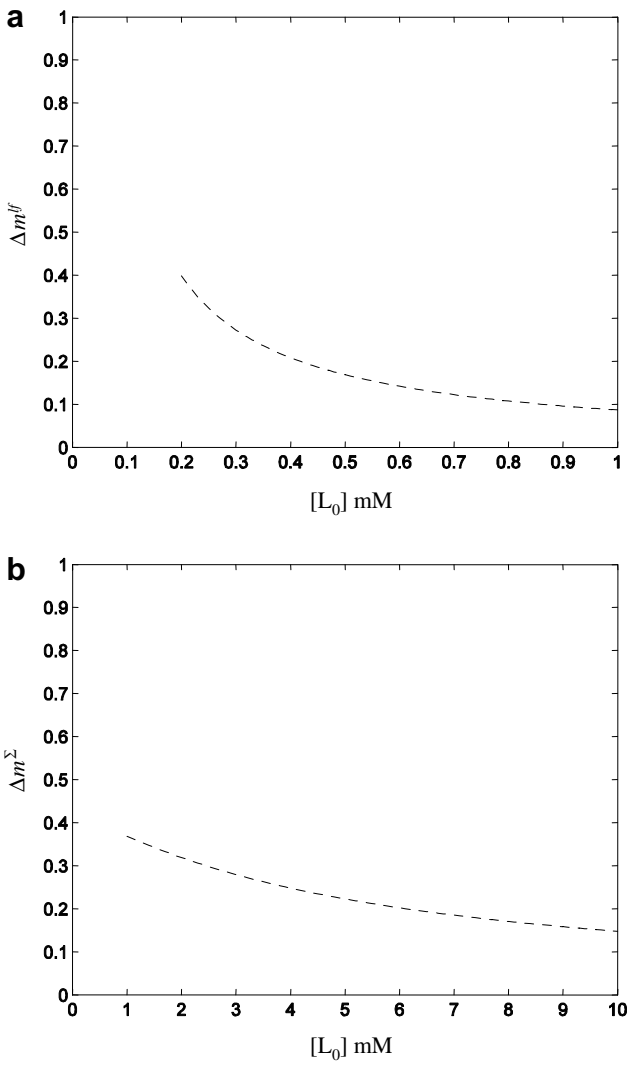

Fig. 4. Magnitude of the NOE-exchange-relay effect ('dip depth') as a function of ligand concentration. Simulated using Eqs. (4.1) and (4.2) with relaxation coefficients as evaluated for the MBG-agglutinin system (same as in Fig. 3b), assuming protein concentration $[\mathrm{P}_0] = 0.1$ mM, on-rate $k_{\mathrm{on}} = 10^8\ \mathrm{M}^{-1}\ \mathrm{s}^{-1}$, and K_{d} of (a) 10 nM or (b) 1 mM. The simulations included the effect of T_2 filters modeled along the lines of Eqs. (4.1) and (4.2) as described in Section 3. The magnitude of the NOE-exchange-relay effect was quantified via $\Delta m^{\mathrm{lf}} = \max_i\{(m_i^{\mathrm{lf}}(0) - m_i^{\mathrm{lf}}(\tau_{\mathrm{mix}}^{\mathrm{min}}))/m_i^{\mathrm{lf}}(\infty)\}$ in the case of the slow exchange (a) and $\Delta m^{\Sigma} = \max_i\{(m_i^{\Sigma}(0) - m_i^{\Sigma}(\tau_{\mathrm{mix}}^{\mathrm{min}}))/m_i^{\Sigma}(\infty)\}$ in the case of the fast exchange (b). Here $m_i(\tau_{\mathrm{mix}}^{\mathrm{min}})$ is the lowest point in the curve, cf. Fig. 3b.

for the leads with higher binding affinity generated at the advanced stages of the drug development process. The experiment is practical so long as the association rate is not much slower than the relaxation rate of the free ligand. It ceases to be useful for tightly binding ligands when $k \approx k_{\mathrm{off}}[\mathrm{P}_0]/([\mathrm{L}_0] - [\mathrm{P}_0]) \ll I^{\mathrm{lf}}$.

7. Concluding remarks

We present here a simple variant of the 1D homonuclear pulse sequence to study binding of ligands to macromolecular targets. Our experiment shares conceptual underpinnings

with the reverse NOE pumping [8] and saturation transfer difference [7,40] techniques. All three schemes produce similar spectra with approximately the same sensitivity, Fig. S1. The standard methods are, however, prone to the usual hazards of differential spectroscopy. For instance, the reverse NOE pumping scheme with (appropriately) long τ_{mix} fails to eliminate the background signal of agglutinin. This is a consequence of the asymmetric placement of the T_2 filter in the pulse sequence. For the same reason, subtraction of the signals from non-binding ligands can be less than perfect. In the STD measurement, the artefacts could in principle emerge if the resonances of the free ligand are inadvertently touched by the saturation pulses. On the other hand, the discussed transient NOE-exchange-relay sequence provides an unmistakable signature of the ligand binding in a form of the characteristic 'dip'. In implementing this pulse sequence, we have tested a new version of the relaxation filter termed 'selective T_1 filter'. This element takes advantage of large selective T_1 relaxation rates in big proteins and, under favorable circumstances, allows for uniform inversion of the protein spectrum (while leaving the magnetization of free ligand untouched).

Based on the complete relaxation and exchange matrix analysis, we developed a simplified model which applies to a broad class of NOE-exchange-relay experiments. The physical meaning of this model is transparent: in addition to conventional relaxation and exchange terms, it also accounts for coupling of ligand magnetization to the protein spin bath via intermolecular NOE within the complex. The treatment so formulated has been used to investigate the applications of the NOE-exchange-relay experiments under different exchange regimes. The systems with fast exchange (typically encountered at the early stages of the drug development process) have been a subject of much NMR work in the past. In contrast, the systems with slow exchange have received little attention. We demonstrated the application of the NOE-exchange-relay experiment to the system of Me-β-D-galactopyranoside in complex with peanut agglutinin which falls in the slow exchange category. It is anticipated that such measurements can be useful for validation of the binding events for high-affinity ligands.

Acknowledgments

We thank Dr. Philip Hajduk of Abbott Laboratories for helpful discussions and Jun Xu for help with experimental measurements. This work was supported by NSF CAREER Grant 044563 to N.R.S.

Appendix A. Supplementary data

One figure showing the spectra of MBG-agglutinin sample recorded with the transient NOE-exchange-relay experiment, reverse NOE pumping experiment, and saturation transfer difference experiment. Supplementary data associated with this article can be found, in the online version, at doi:10.1016/j.jmr.2007.02.016.

References

[1] B.J. Stockman, C. Dalvit, NMR screening techniques in drug discovery and drug design, Prog. NMR Spectrosc. 41 (2002) 187–231.
[2] B. Meyer, T. Peters, NMR spectroscopy techniques for screening and identifying ligand binding to protein receptors, Angew. Chem. Int. Ed. 42 (2003) 864–890.
[3] J.W. Peng, J. Moore, N. Abdul-Manan, NMR experiments for lead generation in drug discovery, Prog. NMR Spectrosc. 44 (2004) 225–256.
[4] C.H. Sun, P.J. Hajduk, Nuclear magnetic resonance in target profiling and compound file enhancement, Curr. Opin. Drug Disc. 9 (2006) 463–470.
[5] S.L. Gordon, K. Wüthrich, Transient proton–proton Overhauser effects in horse ferrocytochrome *C*, J. Am. Chem. Soc. 100 (1978) 7094–7096.
[6] F.W. Dahlquist, K.J. Longmuir, R.B. Du Vernet, Direct observation of chemical exchange by a selective pulse NMR technique, J. Magn. Reson. 17 (1975) 406–410.
[7] M. Mayer, B. Meyer, Characterization of ligand binding by saturation transfer difference NMR spectroscopy, Angew. Chem. Int. Ed. 38 (1999) 1784–1788.
[8] A.D. Chen, M.J. Shapiro, NOE pumping. 2. A high-throughput method to determine compounds with binding affinity to macromolecules by NMR, J. Am. Chem. Soc. 122 (2000) 414–415.
[9] S.D. Wolff, R.S. Balaban, Magnetization transfer contrast (MTC) and tissue water proton relaxation in vivo, Magn. Reson. Med. 10 (1989) 135–144.
[10] R.M. Henkelman, G.J. Stanisz, S.J. Graham, Magnetization transfer in MRI: a review, NMR Biomed. 14 (2001) 57–64.
[11] J.W. Keepers, T.L. James, A theoretical study of distance determinations from NMR: two-dimensional nuclear Overhauser effect spectra, J. Magn. Reson. 57 (1984) 404–426.
[12] H.N.B. Moseley, E.V. Curto, N.R. Krishna, Complete relaxation and conformational exchange matrix (CORCEMA) analysis of NOESY spectra of interacting systems: two-dimensional transferred NOESY, J. Magn. Reson. Ser. B 108 (1995) 243–261.
[13] V. Jayalakshmi, N.R. Krishna, Complete relaxation and conformational exchange matrix (CORCEMA) analysis of intermolecular saturation transfer effects in reversibly forming ligand-receptor complexes, J. Magn. Reson. 155 (2002) 106–118.
[14] A.H. Siriwardena, F. Tian, S. Noble, J.H. Prestegard, A straightforward NMR-spectroscopy-based method for rapid library screening, Angew. Chem. Int. Ed. 41 (2002) 3454–3457.
[15] C. Dalvit, M. Flocco, S. Knapp, M. Mostardini, R. Perego, B.J. Stockman, M. Veronesi, M. Varasi, High-throughput NMR-based screening with competition binding experiments, J. Am. Chem. Soc. 124 (2002) 7702–7709.
[16] V. Sklenar, M. Piotto, R. Leppik, V. Saudek, Gradient-tailored water suppression for ^{1}H–^{15}N HSQC experiments optimized to retain full sensitivity, J. Magn. Reson. Ser. A 102 (1993) 241–245.
[17] E. Kupce, J. Boyd, I.D. Campbell, Short selective pulses for biochemical applications, J. Magn. Reson. Ser. B 106 (1995) 300–303.
[18] K. Pervushin, B. Vogeli, A. Eletsky, Longitudinal ^{1}H relaxation optimization in TROSY NMR spectroscopy, J. Am. Chem. Soc. 124 (2002) 12898–12902.
[19] N.R. Skrynnikov, to be published.
[20] A. Kalk, H.J.C. Berendsen, Proton magnetic relaxation and spin diffusion in proteins, J. Magn. Reson. 24 (1976) 343–366.
[21] B.D. Sykes, W.E. Hull, G.H. Snyder, Experimental evidence for role of cross-relaxation in proton nuclear magnetic resonance spin lattice relaxation time measurements in proteins, Biophys. J. 21 (1978) 137–146.
[22] J.H. Noggle, R.E. Schirmer, The Nuclear Overhauser Effect, Academic Press, New York, 1971.

[23] I. Solomon, Relaxation processes in a system of two spins, Phys. Rev. 99 (1955) 559–565.
[24] H.M. McConnell, Reaction rates by nuclear magnetic resonance, J. Chem. Phys. 28 (1958) 430–431.
[25] K.J. Neurohr, N.M. Young, I.C.P. Smith, H.H. Mantsch, Kinetics of binding of methyl α- and β-D-galactopyranoside to peanut agglutinin: a carbon-13 nuclear magnetic resonance study, Biochemistry 20 (1981) 3499–3504.
[26] R. Lotan, E. Skutelsky, D. Danon, N. Sharon, Purification, composition, and specificity of anti-T lectin from peanut (*Arachis hypogaea*), J. Biol. Chem. 250 (1975) 8518–8523.
[27] NMR Suite. Processing reference manual, Bruker BioSpin GmbH, 2003.
[28] R. Ravishankar, K. Suguna, A. Surolia, M. Vijayan, Structures of the complexes of peanut lectin with methyl-β-galactose and *N*-acetyllactosamine and a comparative study of carbohydrate binding in Gal/GalNAc-specific legume lectins, Acta Cryst. D 55 (1999) 1375–1382.
[29] HyperChem computational chemistry, HyperCube Inc., 1996.
[30] T.S. Ulmer, I.D. Campbell, J. Boyd, The effects of dissolved oxygen upon amide proton relaxation and chemical shift in a perdeuterated protein, J. Magn. Reson. 157 (2002) 181–189.
[31] G. Batta, J. Gervay, Solution-phase ^{13}C and ^{1}H chemical shift anisotropy of sialic acid and its homopolymer (colominic acid) from cross-correlated relaxation, J. Am. Chem. Soc. 117 (1995) 368–374.
[32] L.E. Kay, D.A. Torchia, The effects of dipolar cross-correlation on ^{13}C methyl carbon T_1, T_2, and NOE measurements in macromolecules, J. Magn. Reson. 95 (1991) 536–547.
[33] N.R. Skrynnikov, O. Millet, L.E. Kay, Deuterium spin probes of side-chain dynamics in proteins. 2. Spectral density mapping and identification of nanosecond time-scale side-chain motions, J. Am. Chem. Soc. 124 (2002) 6449–6460.
[34] P. Dais, A.S. Perlin, A ^{13}C spin–lattice relaxation study of solvent effects on the rotational dynamics of methyl glucosides, Carbohydr. Res. 194 (1989) 288–295.
[35] V.A. Daragan, K.H. Mayo, Motional model analyses of protein and peptide dynamics using ^{13}C and ^{15}N NMR relaxation, Prog. NMR Spectrosc. 31 (1997) 63–105.
[36] N.R. Krishna, V. Jayalakshmi, Complete relaxation and conformational exchange matrix analysis of STD-NMR spectra of ligand-receptor complexes, Prog. NMR Spectrosc. 49 (2006) 1–25.
[37] T. Carlomagno, Ligand-target interactions: what can we learn from NMR? Annu. Rev. Biophys. Biomol. Struct. 34 (2005) 245–266.
[38] R. Ishima, S. Shibata, K. Akasaka, General features of proton longitudinal relaxation in proteins in solution, J. Magn. Reson. 91 (1991) 455–465.
[39] L.K. Nicholson, L.E. Kay, D.M. Baldisseri, J. Arango, P.E. Young, A. Bax, D.A. Torchia, Dynamics of methyl groups in proteins as studied by proton-detected ^{13}C NMR spectroscopy: application to the leucine residues of staphylococcal nuclease, Biochemistry 31 (1992) 5253–5263.
[40] C. Dalvit, P. Pevarello, M. Tato, M. Veronesi, A. Vulpetti, M. Sundstrom, Identification of compounds with binding affinity to proteins via magnetization transfer from bulk water, J. Biomol. NMR 18 (2000) 65–68.